# A GLRT Approach to Data-Aided Timing Acquisition in UWB Radios—Part I: Algorithms

Zhi Tian, *Member, IEEE*, and Georgios B. Giannakis, *Fellow, IEEE*

***Abstract*—Realizing the great potential of impulse radio communications depends critically on the success of timing acquisition. To this end, optimum data-aided (DA) timing offset estimators are derived in this paper based on the maximum likelihood (ML) criterion. Specifically, generalized likelihood ratio tests (GLRTs) are employed to detect an ultrawideband (UWB) waveform propagating through dense multipath and to estimate the associated timing and channel parameters in closed form. Capitalizing on the pulse repetition pattern, the GLRT boils down to an amplitude estimation problem, based on which closed-form timing acquisition estimates can be obtained without invoking any line search. The proposed algorithms only employ digital samples collected at a low symbol rate, thus reducing considerably the implementation complexity and acquisition time. Analytical acquisition performance bounds and corroborating simulations are also provided.**

***Index Terms*—Data-aided acquisition, generalized likelihood ratio test, timing recovery, ultrawideband communications.**

## I. Introduction

RESEARCH on ultrawideband (UWB) communications is burgeoning for its envisioned applications on high-speed short-range wireless access, with capability to overlay existing channelized RF services [1], [2]. UWB impulse radios transmit a stream of ultrashort pulses (on the order of subnanoseconds) at very low power density. To maintain adequate signal energy for reliable detection, each information-bearing symbol is transmitted over a large number of frames with one pulse per frame. The frame duration is much larger than the pulse duration, resulting in a low duty cycle UWB transmission.

Implementation of UWB radios has been perplexed by the difficulty in synchronization due to ultrashort low-duty-cycle pulses operating at very low power density. Timing recovery is required not only at the frame level to find when the first frame in each symbol starts but also at the pulse level to find where a pulse is located within a frame. Conventional sliding-correlation-based synchronizers require a long search time and an unreasonably high sampling rate at several gigahertz [3]. The complexity issue is further exacerbated by the performance degradation incurred by dense multipath propagation, especially when time hopping (TH) is used for smoothing the transmit spectrum and for enabling multiple access [1]. Without properly accounting for the unique features of UWB transmissions, synchronization methods that are well suited for narrowband systems are no longer effective. Recent works have focused on obtaining low-complexity algorithms for rapid timing acquisition by making use of coarse bin search [4]–[6] and exploiting coded beacon sequences in conjunction with a correlator bank [8] or subspace-based spectral estimation [9], [10]. Capitalizing on the cyclostationarity naturally present in UWB signaling, non-DA timing acquisition is also possible [11], [12]. Based on the maximum likelihood (ML) criterion, parameter estimation (including tap gains and delays) of UWB multipath channels in the presence of multiple-access interference (MAI) was pursued in [13]. As this ML timing estimator has to operate at a high (subpulse) rate, it is computationally prohibitive for timing acquisition. Relying on a special pilot symbol pattern, a rapid synchronizer was developed recently using frame-rate cross-correlation samples of neighboring noisy received waveforms [17].

In this paper, we develop a data-aided (DA) ML estimation approach, where only symbol-rate samples are needed for timing acquisition. Starting with the no-TH case, we derive a generalized likelihood ratio test (GLRT) for joint detection and frame-level timing acquisition, where channel-dependent unknowns are regarded as nuisance parameters. Interestingly, frame-level timing offset acquisition amounts to an amplitude estimation problem accepting a closed-form solution. Based on symbol-rate samples, the GLRT yields channel-dependent amplitude estimates, the timing acquisition solution, the symbol detection rule, as well as the associated estimation performance bounds. The GLRT reveals that the training symbol sets required for estimating channel-dependent parameters and for acquiring timing information should be nonoverlapping. Judicious design of training sequences is desired also to optimize the overall system performance—a goal that we will pursue in a companion paper [15].

Next, we extend our results to the TH case by properly selecting a noisy template to generate correlator output samples. Such a template inherently accounts for the unknown TH pattern under mistiming, thus being able to retain the desired symbol-rate sample structure that links timing offset parameters with amplitude scaling factors. Use of a noisy template also enjoys effective multipath energy capture and asymptotically maximizes the received signal-to-noise ratio (SNR), which in

Manuscript received January 19, 2004; revised April 25, 2004; accepted August 31, 2004. The editor coordinating the review of this paper and approving it for publication is G. M. Vitetta. The work of Z. Tian was supported by the National Science Foundation (NSF) under Grant CCR-0238174. The work of G. B. Giannakis was supported by the ARL/CTA under Grant DAAD19-01-2-011 and by NSF-ITR under Grant EIA-0324864. This paper was presented in part at the 2003 IEEE Conference on Ultra Wideband Systems and Technologies (UWBST'2003), Reston, VA, November 2003.

Z. Tian is with the Department of Electronics and Communications Engineering, Michigan Technological University, Houghton, MI 49931 USA (e-mail: ztian@mtu.edu).

G. B. Giannakis is with the Department of Electronics and Communications Engineering, University of Minnesota, Minneapolis, MN 55455 USA (e-mail: georgios@ece.umn.edu).

Digital Object Identifier 10.1109/TWC.2005.858356

turn improves timing accuracy, even for UWB radios that do not employ TH.

The rest of the paper is organized as follows. Section II describes a general-form symbol-rate discrete-time UWB signal model with timing offset. In Section III, the timing acquisition problem is formulated as a GLRT, treating the aggregate discrete-time channel-dependent gains as deterministic nuisance parameters. The GLRT solution to timing acquisition is extended to the TH case in Section IV, where a noisy template is adopted to capture adequate multipath energy and to enable timing estimation that is robust to TH. Simulations are presented in Section V for different algorithms under various operating environments to demonstrate their mean-square timing estimation errors and their system-level impact on bit error rate (BER) performance. The paper concludes with summarizing remarks in Section VI.

## II. Signal Model

In UWB impulse radios, every symbol is transmitted using $N_f$ pulses over $N_f$ frames[1] with one pulse per frame. Every frame contains $N_c$ chips. The symbol waveform of duration $T_s := T_f N_f$ is $p_s(t) = \sum_{j=0}^{N_f-1} p(t - jT_f - c_j T_c)$[2], where $p(t)$ is an ultrashort (so-called monocycle) pulse of width $T_p$ at the nanosecond scale, $T_f$ is the frame duration that may be a hundred to a thousand times $T_p$, $T_c := T_f/N_c$ is the chip duration, and the chip sequence $\{c_j\}$ represents the user's pseudo-random TH code with $c_j \in [0, N_c - 1],\ \forall j \in [0, N_f - 1]$. The pulse amplitude is scaled to satisfy $\int p^2(t)dt = 1/N_f$, such that the symbol waveform has unit energy $\int p_s^2(t)dt = 1$. We focus on pulse amplitude modulation (PAM) [2], where the information-bearing symbols $s[n] \in \{\pm 1\}$ are modeled as binary independent and identically distributed with energy $\mathcal{E}_s$ spread over $N_f$ frames. The transmitted UWB waveform is then given by [see also Figs. 1(a) and 2(a) for an example with $N_f = 3$]

$$u(t) = \sqrt{\mathcal{E}_s} \sum_{n=-\infty}^{\infty} s[n] p_s(t - nT_s). \tag{1}$$

The signal $u(t)$ propagates through an $L$-path fading channel, with $\{\alpha_l\}$ and $\{\tau_l\}$ representing the attenuation and the delay of the $l$th path, respectively, and $\tau_0 < \tau_1 < \cdots < \tau_{L-1}$. Timing information of interest refers to the first arriving time $\tau_0$, which is measured with reference to the receiver's local clock. From this perspective, we isolate $\tau_0$ and model the channel impulse response as a summation $\sum_{l=0}^{L-1} \alpha_l \delta(t - \tau_{l,0})$, where $\tau_{l,0} := \tau_l - \tau_0$ is the relative time delay of each path. The channel delay spread $\tau_{L-1,0}$ stays within a frame since we select $T_f \geq \tau_{L-1,0} + T_p + (c_{N_f-1} - c_0)T_c$ to avoid intersymbol interference [Fig. 1(b)]. The composite channel expressed as the convolution of the multipath with the transmitted pulse $p(t)$ is given by $g(t) = \sum_{l=0}^{L-1} \alpha_l p(t - \tau_{l,0})$, and the time-dispersed received symbol waveform of duration $T_s$ becomes

$$g_s(t) = \sum_{j=0}^{N_f-1} g(t - jT_f - c_j T_c) = \sum_{l=0}^{L-1} \alpha_l p_s(t - \tau_{l,0}) \tag{2}$$

as illustrated in Fig. 1(b) for the no-TH case and in Fig. 2(b) for the TH case with TH-induced interframe interference (IFI). The receive waveform is thus given by

$$\begin{aligned} r(t) &= \sum_{l=0}^{L-1} \alpha_l u(t - \tau_0 - \tau_{l,0}) + w(t) \\ &= \sqrt{\mathcal{E}_s} \sum_{n=-\infty}^{\infty} s[n] g_s(t - nT_s - \tau_0) + w(t) \end{aligned} \tag{3}$$

where the wide sense stationary process $w(t)$ accounts for both thermal noise and MAI, which similar to [7] is approximated as white Gaussian. Letting $\lfloor \cdot \rfloor$ denote integer floor, we dissect $\tau_0$ based on different time scales and express it as $\tau_0 := n_s T_s + n_f T_f + \epsilon$, where $n_s := \lfloor \tau_0/T_s \rfloor$ denotes the symbol-level offset, $n_f := \lfloor (\tau_0 - n_s T_s)/T_f \rfloor \in [0, N_f - 1]$ the frame-level offset, and $\epsilon \in [0, T_f)$ the pulse-level offset, respectively. These different levels of timing offsets are illustrated in Fig. 1 via an example where $\tau_0 = (n_s = 0)T_s + (n_f = 1)T_f + (\epsilon = 2T_f/3)$, with $N_f = 3$. Using these definitions and (1), the received signal can be expressed by

$$r(t) = \sqrt{\mathcal{E}_s} \sum_{n=-\infty}^{\infty} s[n] g_s(t - nT_s - n_s T_s - n_f T_f - \epsilon) + w(t). \tag{4}$$

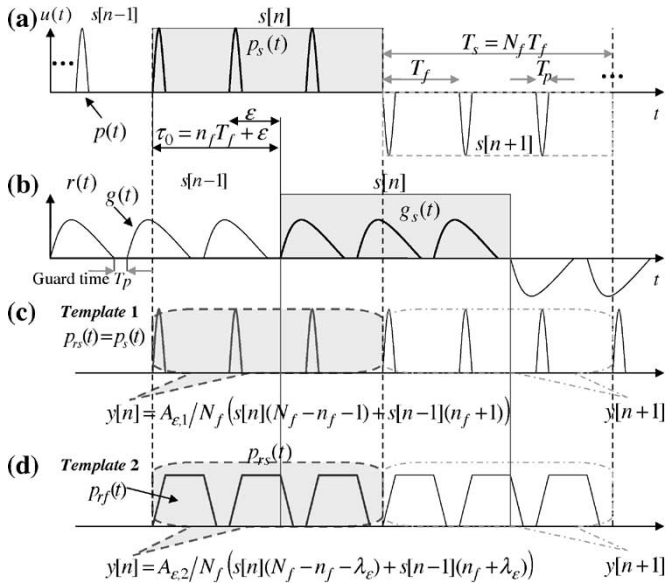


Fig. 1. Transmit/receive waveforms and symbol templates in the TH-free case: $n_s = 0$, $n_f = 1$, and $N_f = 3$. Dashed vertical lines represent symbol boundaries in the transmitted waveform and the correlation template, while solid vertical lines represent symbol boundaries in the received waveform.

[1]Spreading a single symbol over $N_f$ frames in the UWB case reverses the commonly used terminology where a frame consists of multiple symbols.

[2]Throughout the paper, we will use the subscript $s$ to refer to symbol-related variables, such as symbol duration, symbol waveforms, symbol-level timing offset, and symbol-long correlation templates. Similarly, we will use the subscripts $f$ and $r$ to denote frame- and receiver-related quantities.

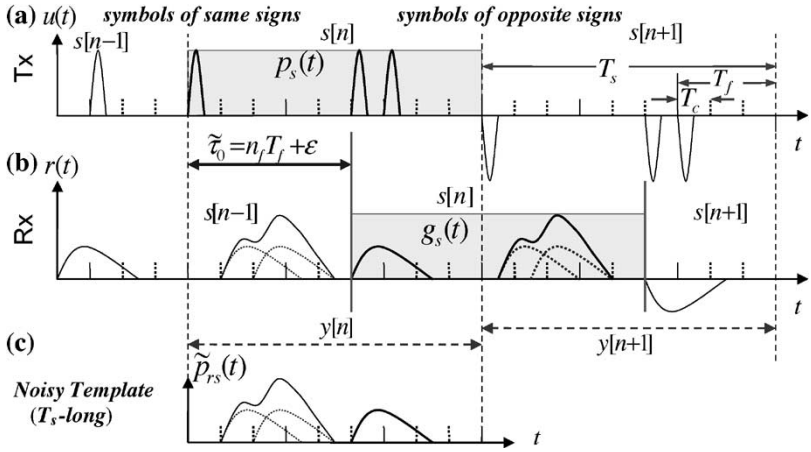


Fig. 2. Transmit/receive waveforms and the ideal/noisy template in the TH case (noise-free): $n_s = 0$, $n_f = 1$, $N_f = 3$, $T_c = T_f/3$, and the TH code $\{c_j\}_{j=0}^{N_f-1}$ for each symbol is [0,2,0]. Dashed pulses in (b) are the received $g(t)$ after channel distortion, and solid pulses are the composite $g_s(t)$ after mixing TH-shifted $g(t)$s.

A symbol-by-symbol sliding correlator is applied to generate samples $y[n]$ at the symbol rate by

$$y[n] := \int_0^{T_s} r(t + nT_s) p_{rs}(t) dt \tag{5}$$

where $p_{rs}(t), t \in [0, T_s]$ is the correlation template. The choice of the template $p_{rs}(t)$ affects detection performance and its robustness to mistiming. A simple template corresponds to $p_{rs}(t) = p_s(t)$, whereas the ideal template under perfect timing and channel knowledge is given by $p_{rs}(t) = g_s(t)$, which is equivalent to maximum ratio combining. In the presence of dense multipath, the choice of $p_{rs}(t)$ affects the received energy captured in discrete-time samples $\{y[n]\}$, which in turn influences the timing offset estimation accuracy of our digital synchronizers.

Given $N$ samples $\{y[n]\}_{n=0}^{N-1}$, our goal in this paper is to acquire timing by optimally estimating $n_s$ and $n_f$ based on $M$ training symbols $\{s[n]\}_{n=0}^{M-1}$—a DA digital timing acquisition problem.

## III. GLRT-Based Synchronization Approach

For clarity, we first consider a point-to-point link where no TH is employed, i.e., $\{c_j = 0\}$, and derive optimum acquisition rules using the GLRT (see, e.g., [18, Ch. 6]). The results will be extended to include TH in the next section.

### A. Discrete-Time Signal Model Under Mistiming

Under perfect timing ($\tau_0 = 0$), each sample $y[n]$ of the correlator output serves as the detection statistic for a single symbol $s[n]$. With mistiming ($\tau_0 \neq 0$), however, $y[n]$ depends on two consecutive symbols as depicted in Fig. 1(c) and (d) [for clarity we set $n_s = 0$ in Fig. 1(b)]. The time indices of the two contributing symbols are determined by the symbol-level offset $n_s T_s$, whereas portions of the corresponding two transmitted symbol waveforms depend on the frame-level offset $n_f T_f$. We quantify these effects in Appendix A and establish the resulting sampled model in the following proposition.

*Proposition 1:* For a general receive correlator template $p_{rs}(t) = \sum_{j=0}^{N_f-1} p_{rf}(t - jT_f)$ of duration $T_s$ with $p_{rf}(t)$ having nonzero support $T_{rf} \leq T_f$, the symbol-rate sampled output $y[n]$ in the no-TH case is given by

$$y[n] = A_\epsilon \left(s[n - n_s](N_f - n_f - \lambda_\epsilon) + s[n - n_s - 1](n_f + \lambda_\epsilon)\right) + w[n] \tag{6}$$

where $A_\epsilon := \sqrt{\mathcal{E}_s} \int_0^{T_f} g_s(t + T_f - \epsilon) p_{rf}(t) dt = \sqrt{\mathcal{E}_s} \int_\epsilon^{T_f} g(t - \epsilon) p_{rf}(t) dt + \sqrt{\mathcal{E}_s} \int_0^{\epsilon} g(t + T_f - \epsilon) p_{rf}(t) dt$ is independent of $n_s$ and $n_f$, and $\lambda_\epsilon := (1/A_\epsilon)\sqrt{\mathcal{E}_s} \int_0^{\epsilon} g(t + T_f - \epsilon) p_{rf}(t) dt$ is bounded within [0,1]. The sample $w[n]$ denotes additive white Gaussian noise (AWGN) with zero mean. Furthermore

1) if $s[n - n_s] = s[n - n_s - 1]$, then (6) reduces to $y[n] = A_\epsilon N_f s[n - n_s] + w[n]$;
2) if $s[n - n_s] = -s[n - n_s - 1]$, then $y[n] = A_\epsilon(N_f - 2\nu_{f,\epsilon}) s[n - n_s] + w[n]$, where $\nu_{f,\epsilon} := n_f + \lambda_\epsilon \approx \tilde{\tau}_0/T_f$;
3) if $p_{rf}(t) = p(t)$ and $T_f \geq \tau_{L-1,0} + 2T_p$, then $\nu_{f,\epsilon} = n_f, \forall \epsilon$.

Proposition 1 clearly establishes the effects of different levels of timing offset on the symbol-rate correlator output $y[n]$. When two consecutive symbols have the same sign as in 1), the corresponding $y[n]$ contains no information about $n_f$. However, the channel-dependent amplitude $A_\epsilon$ can be estimated from $y[n]$ samples obeying 1) in the ML sense and the resulting $\hat{A}_\epsilon$ can be used in 2) to recover $\tilde{\tau}_0$ and $n_f$ as $\hat{\tilde{\tau}}_0 \approx \hat{\nu}_{f,\epsilon} T_f$ and $\hat{n}_f = \lfloor \hat{\nu}_{f,\epsilon} \rfloor$ since $\lambda_\epsilon \in [0, 1]$. Estimation of $n_f$ depends on the choice of the frame-level template $p_{rf}(t)$. When the conventional $p_{rf}(t) = p(t)$ is used [cf. Fig. 1(c)] and the frame length $T_f$ is suitably selected to include an extra guard time $T_p$ in addition to the spread of the aggregate channel $g(t)$ [cf. Fig. 1(b)], it follows from 3) that estimating $\nu_{f,\epsilon}$ from 2) in the ML sense is identical to computing the ML estimate of $n_f$. However, as will become clear later on, estimation

performance can be improved with a general $p_{rf}(t)$ of width $T_{rf} > T_p$ [e.g., the trapezoidal template shown in Fig. 1(d)]. In this case, we will pursue the ML estimate of $\nu_{f,\epsilon}$ based on 2) and subsequently estimate $n_f$ as $\lfloor \hat{\nu}_{f,\epsilon} \rfloor$.

### B. Formulation as a Hypothesis Testing Problem

Building on Proposition 1, we now pursue estimation of both the symbol-level timing offsets $n_s$ and $\nu_{f,\epsilon}$ that contain the frame-level timing offset $n_f$. Suppose that a total of $M$ training symbols $\{s[n]\}_{n=0}^{M-1}$ are received during $[\tau_0, \tau_0 + MT_s]$. Without knowing when the UWB stream starts, a synchronizer collects $N$ observations $\mathbf{y} := [y[0], \ldots, y[N-1]]^T$ over the interval $[0, NT_s]$. We formulate the following binary hypothesis testing problem for detecting $y[n]$ along with estimating $n_s$ and $\nu_{f,\epsilon}$, i.e.,

$$H_1 : y[n] = A_\epsilon (s[n-n_s](N_f - \nu_{f,\epsilon}) + s[n-n_s-1]\nu_{f,\epsilon}) + w[n], \quad n = n_s, \ldots, n_s + M - 1 \le N-1 \tag{7}$$

$$H_0 : y[n] = w[n], \quad n = 0, 1, \ldots, N-1. \tag{8}$$

Here, $s[n]$ is deterministic and known, $A_\epsilon$, $\nu_{f,\epsilon}$, and $n_s$ are unknown nuisance parameters, and $w[n]$ has variance $\sigma_w^2$. This is a classical detection problem with unknown parameters in AWGN, for which the GLRT is well motivated. Utilizing the probability density function (pdf) $p(\cdot)$ of $\mathbf{y}$ conditioned on the two hypotheses, the GLRT rejects $H_0$ if

$$J_0(\mathbf{y}; A_\epsilon, \nu_{f,\epsilon}, n_s) := \frac{p(\mathbf{y}; \hat{A}_\epsilon, \hat{\nu}_{f,\epsilon}, \hat{n}_s, H_1)}{p(\mathbf{y}; H_0)} \ge \tau_{FA} \tag{9}$$

where $\hat{A}_\epsilon$, $\hat{\nu}_{f,\epsilon}$, and $\hat{n}_s$ are the corresponding ML estimates (MLEs) under $H_1$, and $\mathcal{T}_{FA}$ is a threshold set by the desired probability of false alarms (FA). When seeking MLEs of the unknown parameters, we not only assume that $\nu_{f,\epsilon}$ and $n_s$ are deterministic but also treat the channel-dependent amplitude $A_\epsilon$ as deterministic but unknown, which leads to a conditional ML (CML) approach [20]. In contrast, an unconstrained ML regards the unknown $A_\epsilon$ as a random variable, which leads to $\hat{A}_\epsilon$ estimators that depend on the underlying channel statistics.

Before proceeding with the GLRT, it is appropriate to clarify the role of the training sequence (TS) pattern in this hypothesis-testing problem. The correlator output samples under $H_1$, denoted as $\mathbf{y}_s := \{y[n] : y[n] \in H_1\} = [y[n_s], \ldots, y[n_s + M - 1]]^T$, clearly depend on $n_s$. For binary PAM, $\mathbf{y}_s$ can be split into two groups: one group, denoted by $\mathbf{y}_+(n_s) := \{y[n] : n \in \mathcal{G}_+(n; n_s)\}$, is indexed by all the $n$s in the set $\mathcal{G}_+(n; n_s) := \{n : s[n-n_s] = s[n-n_s-1]\}$, while the second group, $\mathbf{y}_-(n_s) := \{y[n] : n \in \mathcal{G}_-(n; n_s)\}$, is associated with the rest of $n$s in the set $\mathcal{G}_-(n; n_s) := \{n : s[n-n_s] = -s[n-n_s-1]\}$. For a given $n_s$, this partitioning into two nonoverlapping sets $\mathcal{G}_+(n; n_s)$ and $\mathcal{G}_-(n; n_s)$ is solely determined by whether the two successive symbols involved in the correlator output under mistiming [cf. (6)] have identical or opposite signs. The two data sets have sizes $M_+ := |\mathcal{G}_+(n; n_s)|$ and $M_- := |\mathcal{G}_-(n; n_s)|$, respectively, which obviously depend on the TS pattern, but not on the symbol offset $n_s$. Depending on whether $s[n] = s[n-1]$ or $s[n] = -s[n-1]$, $H_1$ in (7) can be rewritten as

$$H_1 : y[n] = \begin{cases} A_\epsilon N_f s[n] + w[n], & n \in \mathcal{G}_+(n; n_s) \\ A_\epsilon (N_f - 2\nu_{f,\epsilon}) s[n] + w[n], & n \in \mathcal{G}_-(n; n_s). \end{cases} \tag{10}$$

Since $\mathbf{y}_+(n_s)$ does not contain $\nu_{f,\epsilon}$, it will not play a role in finding the MLE $\hat{\nu}_{f,\epsilon}$. On the other hand, for any $y[n] \in \mathbf{y}_-(n_s)$, the channel-dependent parameter $A_\epsilon$ and the frame-level timing parameter $\nu_{f,\epsilon}$ are always coupled in a nonidentifiable manner. Indeed, the true pair $(A_\epsilon, \nu_{f,\epsilon})$ and another pair $(cA_\epsilon, ((c-1)N_f + 2\nu_{f,\epsilon})/2c)$, with any $c \ge 1 - 2\nu_{f,\epsilon}/N_f \ge 0$, give rise to the same $\mathbf{y}_-(n_s)$. These observations motivate us to estimate $A_\epsilon$ and $\nu_{f,\epsilon}$ from the two disjoint data sets $\mathbf{y}_+(n_s)$ and $\mathbf{y}_-(n_s)$, separately. Compared with working directly on the entire sample set $\mathbf{y}_s = \mathbf{y}_-(n_s) \bigcup \mathbf{y}_+(n_s)$, this separate approach will retain ML optimality of $\hat{\nu}_{f,\epsilon}$ since we do not disregard any useful data. One may question the optimality of $\hat{A}_\epsilon$ since the unused portion $\mathbf{y}_-(n_s)$ also contains channel-related information. We maintain that $\mathbf{y}_-(n_s)$ does not offer additional information on $A_\epsilon$ since it cannot resolve the ambiguity between $A_\epsilon$ and $(N_f - 2\nu_{f,\epsilon})$ without knowing $\nu_{f,\epsilon}$, which has to be estimated from $\mathbf{y}_-(n_s)$ itself. This optimality claim will be rigorously proved in the following subsection.

### C. CML Timing Acquisition Using Symbol-Rate Samples

With $A_\epsilon$, $n_s$, $\nu_{f,\epsilon}$ being deterministic but unknown and $w[n]$ being AWGN, straightforward manipulation leads to the log-likelihood ratio (LLR)

$$\begin{aligned} &J(\mathbf{y}; A_\epsilon, \nu_{f,\epsilon}, n_s) \\ &= 2\sigma_w^2 \log \frac{p(\mathbf{y}; A_\epsilon, \nu_{f,\epsilon}, n_s, H_1)}{p(\mathbf{y}; H_0)} \\ &= 2A_\epsilon \sum_{n=n_s}^{n_s+M-1} y[n](s[n-n_s](N_f - \nu_{f,\epsilon}) + s[n-n_s-1]\nu_{f,\epsilon}) \\ &\quad - A_\epsilon^2 \sum_{n=n_s}^{n_s+M-1} (s[n-n_s](N_f - \nu_{f,\epsilon}) + s[n-n_s-1]\nu_{f,\epsilon})^2 . \end{aligned} \tag{11}$$

The nuisance parameters in this LLR are $A_\epsilon$, $\nu_{f,\epsilon}$, and $n_s$, whose MLEs will be derived in an alternating fashion. Let us first fix $n_s$ and estimate $A_\epsilon$ from $\mathbf{y}_+(n_s)$ and $\nu_{f,\epsilon}$ from $\mathbf{y}_-(n_s)$, as suggested by the separation property we discussed earlier. The MLE of $n_s$ will then be found after substituting $A_\epsilon$ and $\nu_{f,\epsilon}$ in (11) with their $n_s$-dependent MLEs.

To perform separate ML estimation, we decompose the LLR in (11) into $J(\mathbf{y}; A_\epsilon, \nu_{f,\epsilon}, n_s) = J_+(\mathbf{y}_+(n_s); A_\epsilon, \nu_{f,\epsilon}, n_s) + J_-(\mathbf{y}_-(n_s); A_\epsilon, \nu_{f,\epsilon}, n_s)$, where $J_+(\cdot)$ and $J_-(\cdot)$ consist of the subsets of summands corresponding to $\mathcal{G}_-(n; n_s)$ and

$\mathcal{G}_+(n;n_s)$, respectively. When estimating $A_\epsilon$, only $J_+(\cdot)$ is relevant, which we write as a function of $A_\epsilon$ in the form

$$J_+\left(A_\epsilon;n_s,\mathbf{y}_+(n_s)\right) = 2A_\epsilon N_f \sum_{n\in\mathcal{G}_+(n;n_s)} y[n]s[n-n_s] - \mathcal{E}_M^+ A_\epsilon^2 N_f^2 \quad (12)$$

where $\mathcal{E}_M^+ := \sum_{n\in\mathcal{G}_+(n;n_s)} s^2[n-n_s]$ is the symbol energy corresponding to $\mathbf{y}_+(n_s)$. In a binary transmission, $\mathcal{E}_M^+ = M_+$ equals the cardinality of $\mathcal{G}_+(n;n_s)$, which is independent of $n_s$. The LLR in (12) corresponds to the problem of detecting a deterministic signal known except for its amplitude in AWGN [18]. It is straightforward to find from (12) the MLE of $A_\epsilon$ conditioned on $n_s$, the associated Crameŕ–Rao bound (CRB), and the resulting maximum $J_+(\cdot)$ at the optimum $\hat{A}_\epsilon(n_s)$, all in closed-form

$$\hat{A}_\epsilon(n_s) = \frac{1}{N_f\mathcal{E}_M^+}\sum_{n\in\mathcal{G}_+(n;n_s)} y[n]s[n-n_s] \quad (13)$$

$$\mathrm{CRB}(\hat{A}_\epsilon;n_s) = -\frac{2\sigma_w^2}{\frac{\partial^2 J_+(A_\epsilon;n_s,\mathbf{y}_+(n_s))}{\partial A_\epsilon^2}} = \frac{\sigma_w^2}{N_f^2\mathcal{E}_M^+} \quad (14)$$

$$J_+(n_s;\mathbf{y}_+(n_s)) := J_+\left(n_s;\hat{A}_\epsilon(n_s),\mathbf{y}_+(n_s)\right) = \frac{1}{\mathcal{E}_M^+}\left(\sum_{n\in\mathcal{G}_+(n;n_s)} y[n]s[n-n_s]\right)^2. \quad (15)$$

The $\hat{A}_\epsilon(n_s)$ estimate in (13) takes the usual cross correlation form between the input sequence and the shifted output sequence. The estimation quality, measured by the $\mathrm{CRB}(\hat{A}_\epsilon;n_s)$ in (14), is inversely proportional to the number of training symbols in the set $\mathcal{G}_+(n;n_s)$ as expected, while the resulting maximum LLR in (15) is proportional to the cross-correlation energy.

Moving on to find the MLE of $\nu_{f,\epsilon}$, we focus on $\mathbf{y}_-(n_s)$ and write the corresponding $J_-(\cdot)$ as

$$J_-\left(\nu_{f,\epsilon};A_\epsilon,n_s,\mathbf{y}_+(n_s)\right) = 2A_\epsilon(N_f-2\nu_{f,\epsilon}) \times \sum_{n\in\mathcal{G}_-(n;n_s)} y[n]s[n-n_s] - \mathcal{E}_M^- A_\epsilon^2(N_f-2\nu_{f,\epsilon})^2 \quad (16)$$

where $\mathcal{E}_M^- := \sum_{n\in\mathcal{G}_-(n;n_s)} s^2[n-n_s]$. Since $A_\epsilon$ has been found via (13), the LLR in (16) corresponds to the problem of detecting a deterministic signal known except for the mistiming-dependent scale factor $(N_f-2\nu_{f,\epsilon})$ in AWGN. By maximizing (16), we reach the MLE of $\nu_{f,\epsilon}$ conditioned on $A_\epsilon$ and $n_s$, the associated CRB, and the resulting maximum $J_-(\cdot)$ at the optimum $\hat{\nu}_{f,\epsilon}(n_s)$, also in closed-form

$$\hat{\nu}_{f,\epsilon}(A_\epsilon,n_s) = \frac{N_f}{2} - \frac{1}{2A_\epsilon\mathcal{E}_M^-}\sum_{n\in\mathcal{G}_-(n;n_s)} y[n]s[n-n_s] \quad (17)$$

$$\mathrm{CRB}(\hat{\nu}_{f,\epsilon};A_\epsilon,n_s) = -\frac{2\sigma_w^2}{\frac{\partial^2 J_-(\nu_{f,\epsilon};A_\epsilon,n_s,\mathbf{y}_-(n_s))}{\partial\nu_{f,\epsilon}^2}} = \frac{\sigma_w^2}{4A_\epsilon^2\mathcal{E}_M^-} \quad (18)$$

$$J_-\left(n_s;\mathbf{y}_-(n_s)\right) := J_-\left(n_s;\hat{\nu}_{f,\epsilon}(A_\epsilon,n_s),\mathbf{y}_-(n_s)\right) = \frac{1}{\mathcal{E}_M^-}\left(\sum_{n\in\mathcal{G}_-(n;n_s)} y[n]s[n-n_s]\right)^2. \quad (19)$$

Similar to (13), the $\hat{\nu}_{f,\epsilon}$ estimate in (17) is determined by the cross correlation over the set $\mathcal{G}_-(n;n_s)$, while again the CRB in (18) is inversely proportional to the number of training symbols in this set since $\mathcal{E}_M^- = M_-$. In addition, $\hat{\nu}_{f,\epsilon}$ and its associated conditional CRB also depend on the aggregate channel-dependent parameter $A_\epsilon$. On the other hand, note from (19) that $J_-(\cdot)$ at the optimum $\hat{\nu}_{f,\epsilon}(A_\epsilon,n_s)$ does not depend on $A_\epsilon$. Therefore, no $\hat{A}_\epsilon$ estimate can be obtained from $\mathbf{y}_-(n_s)$ due to the ambiguity between $A_\epsilon$ and $\nu_{f,\epsilon}$. In fact, the overall LLR for optimizing $A_\epsilon$ is the same as $J_+(\cdot)$ induced by $\mathbf{y}_+(n_s)$ because

$$J(A_\epsilon;\hat{\nu}_{f,\epsilon},n_s,\mathbf{y}) = J_+\left(A_\epsilon;\hat{\nu}_{f,\epsilon},n_s,\mathbf{y}_+(n_s)\right) + J_-\left(A_\epsilon;\hat{\nu}_{f,\epsilon},n_s,\mathbf{y}_-(n_s)\right) = J_+\left(A_\epsilon,n_s,\mathbf{y}_+(n_s)\right) + C \quad (20)$$

where $C := J_-(n_s;\mathbf{y}_-(n_s))$ is a constant independent of $A_\epsilon$. Thus, we have proved that the MLE of $A_\epsilon$ based on the entire data set $\mathbf{y}_s$ coincides with that based on $\mathbf{y}_+(n_s)$ only. In fact, a more tedious derivation that directly maximizes (11) with respect to $A_\epsilon$ yields

$$\hat{A}(n_s) = \arg\max_{A_\epsilon} J(A_\epsilon;n_s,\mathbf{y}) = \frac{\sum_{n=n_s}^{n_s+M-1} y[n]\left(s[n-n_s]+s[n-n_s-1]\right)}{N_f\mathcal{E}_M + N_f\sum_{n=n_s}^{n_s+M-1} s[n-n_s]s[n-n_s-1]} \quad (21)$$

where $\mathcal{E}_M := \mathcal{E}_M^+ + \mathcal{E}_M^-$. Seemingly different from the $\hat{A}_\epsilon$ estimate obtained from $\mathbf{y}_+(n_s)$ in (13), the $\hat{A}_\epsilon$ obtained from $\mathbf{y}_s$ in (21) can be reduced to exactly that in (13), utilizing the binary nature of $\{s[n]\}$. In a nutshell, we have established that the separate estimation approach retains ML optimality of $\hat{A}_\epsilon$.

Having obtained the $n_s$-dependent MLEs of $A_\epsilon$ and $\nu_{f,\epsilon}$ in (13) and (17), the next task is to derive the MLE of $n_s$. Note that either $J_+(n_s;\mathbf{y}_+(n_s))$ or $J_-(n_s;\mathbf{y}_-(n_s))$ could serve as an objective function based on which $n_s$ can be estimated using a line search. However, since both $\mathbf{y}_+(n_s)$ and $\mathbf{y}_-(n_s)$ contain useful information about $n_s$, the MLE utilizing all the samples $\mathbf{y}$ should be designed from the LLR in (11), which is nothing but the sum of $J_+(\cdot)$ and $J_-(\cdot)$. Thus, we reach from (15) and (19) the MLE of $n_s$ as

$$\begin{aligned}\hat{n}_s &= \arg\max_{n_s\in[0,N-M]} J(n_s,\mathbf{y}) \\ &= \arg\max_{n_s\in[0,N-M]} \left[J_+\left(n_s;\mathbf{y}_+(n_s)\right)+J_-\left(n_s;\mathbf{y}_-(n_s)\right)\right] \\ &= \arg\max_{n_s\in[0,N-M]} \left[\frac{1}{\mathcal{E}_M^+}\left(\sum_{n\in\mathcal{G}_+(n;n_s)} y[n]s[n-n_s]\right)^2 \right. \\ &\qquad \left. +\frac{1}{\mathcal{E}_M^-}\left(\sum_{n\in\mathcal{G}_-(n;n_s)} y[n]s[n-n_s]\right)^2\right]. \end{aligned} \tag{22}$$

So far, we have obtained the MLEs of all nuisance parameters, where $\hat{A}_\epsilon$ depends on $n_s$ and $\hat{\nu}_{f,\epsilon}$ depends on both $A_\epsilon$ and $n_s$. In implementing our timing algorithm, one should follow these dependencies and proceed in a reverse order to estimate $\hat{n}_s$ first, $\hat{A}_\epsilon$ afterwards, and finally $\hat{\nu}_{f,\epsilon}$, according to (22), (13), and (17). The estimate of $n_f$ itself is then given by the integer floor of $\hat{\nu}_{f,\epsilon}$. The UWB waveform is detected when the optimum LLR exceeds a threshold $\mathcal{T}_{FA}$ predescribed by a desired probability of false alarms $P_{FA}$

$$\text{detection}: J(\hat{n}_s;\mathbf{y}) \geq 2\sigma_w^2 \ln \mathcal{T}_{FA} \tag{23}$$

where $\mathcal{T}_{FA}=\sigma_w Q^{-1}(P_{FA})$ and $Q(x):=(1/\sqrt{2\pi})\int_x^\infty \exp(-u^2/2)du$ denotes the complementary error function.

The implementation advantages of our symbol-rate GLRT timing acquisition approach are evident. In addition to requiring very low sampling rate of one sample per symbol, this approach does not involve discrete-time line search, as most correlation-based synchronizers do at least on a frame-by-frame basis [17]. The frame-level timing offset information manifests in the amplitudes of two TS subsets and is obtained using simple amplitude estimators based on digital cross-correlation operations.

## IV. Robust Timing Recovery With Noisy Template

When TH is employed, the discrete-time model of $y[n]$ in (6) no longer holds true for all templates $p_{rs}(t)$ made of $N_f$ equally spaced replicas of a frame-template $p_{rf}(t)$. Because of the different TH codes used in different frames, each receiver template $p_{rf}(t)$ correlates with a different portion of the TH-dependent aggregate channel $g_s(t)$. As a result, there does not exist a single channel-dependent amplitude $A_\epsilon$ common to all frames. In fact, when the TH codes repeat from symbol to symbol, the channel-dependent $A_\epsilon$ takes on $N_f$ possible values, reflecting the periodicity of the TH codes over frames. As such, the portions of $y[n]$ contributed from two consecutive symbols cannot be simply linked to the acquisition offset parameter $\nu_{f,\epsilon}$, rendering Proposition 1 invalid. On the other hand, Proposition 1 still applies when some properly selected template is used to account for the TH effect. We will present such a template $p_{rs}(t)=\tilde{p}_{rs}(t)$ next and discuss the corresponding asymptotic GLRT timing acquisition solution under TH.

### A. Sample Model for an Ideal Template

With perfect timing ($\tau_0=0$), the ML optimum correlator is a filter matched to the aggregate symbol-long channel $g_s(t)$, which must be known to the receiver. Under mistiming, the optimum symbol-by-symbol correlation template is given by

$$\tilde{p}_{rs}(t)=\begin{cases} g_s(t-\tilde{\tau}_0), & t\in[\tilde{\tau}_0,T_s) \\ g_s(t+T_s-\tilde{\tau}_0), & t\in[0,\tilde{\tau}_0)\end{cases} \tag{24}$$

where $\tilde{\tau}_0:=n_fT_f+\epsilon$ is the timing offset within a symbol period and $\tilde{p}_{rs}(t)$ is nothing but a circularly shifted (by $\tilde{\tau}_0$) version of $g_s(t)$ to confine it within $[0,T_s)$. As depicted in Fig. 2, $\tilde{p}_{rs}(t)$ is in essence the aggregate $T_s$-long channel that is viewed with reference to the receiver's clock; see the $T_s$-apart mistimed symbol boundaries in Fig. 2 (dashed vertical lines) at $t=kT_s$, $\forall k$. On the other hand, $g_s(t)$ can be properly located by the receiver only when $\tilde{\tau}_0$ is known; see the (unknown) actual received symbol boundaries in Fig. 2(b) (solid vertical lines) at $t=\tilde{\tau}_0+kT_s$, $\forall k\geq n_s$.

Because $\tilde{p}_{rs}(t)$ inherently contains the correct TH code in each frame without knowing $\tau_0$, it hops in accordance with the received waveform to correlate with the same portion of $r(t)$ in each frame, subject to the impact of IFI. As a result, the aggregate channel-dependent amplitude $\hat{A}_\epsilon$ is approximately the same for all frames, making (6) approximately valid. We quantify the sample model of $y[n]$ resulting from the use of $p_{rs}(t)=\tilde{p}_{rs}(t)$ in Appendix B and establish the following proposition under TH.

*Proposition 2:* For the correlator template $\tilde{p}_{rs}(t)$ in (24), the symbol-rate sample output $y[n]$ in the presence of TH is given by

$$\begin{aligned} y[n]=A_\epsilon\Big(&s[n-n_s](N_f-n_f-\tilde{\lambda}_\epsilon) \\ &+s[n-n_s-1](n_f+\tilde{\lambda}_\epsilon)\Big)+w[n] \end{aligned} \tag{25}$$

where $A_\epsilon=(\sqrt{\mathcal{E}_s}/N_f)\int_0^{T_s} g_s^2(t)dt\approx\sqrt{\mathcal{E}_s}\int_0^{T_f} g^2(t)dt$ and the bounded $\tilde{\lambda}_\epsilon$ entails the effects of both the pulse-level mistiming $\epsilon$ and the IFI.

Similar to the no-TH case in (6), each sample $y[n]$ is a weighted linear combination of two consecutive symbols, with the combining weights determined by $\nu_{f,\epsilon}:=n_f+\tilde{\lambda}_\epsilon$, whose integer portion corresponds to the frame-level timing offset parameter $n_f$. Accordingly, the channel-dependent unknowns $A_\epsilon$ and $\nu_{f,\epsilon}$ (thus $n_f$) can be obtained via amplitude estimation

in the ML sense provided that $\tilde{p}_{rs}(t)$ is available. However, the ideal $\tilde{p}_{rs}(t)$ contains the channel-related information that is unknown during the synchronization phase. Interestingly, we will see that the receiver can acquire a noisy template $\hat{\tilde{p}}_{rs}(t)$ from the received waveform $r(t)$ that approaches $\tilde{p}_{rs}(t)$ given a sufficient number of training symbols $M$. Based on this noisy template and using $y[n]$ samples as in (25), we will develop a GLRT-based solution to timing acquisition in the presence of TH, starting from the construction of the desired noisy template $\hat{\tilde{p}}_{rs}(t)$.

### B. CML Timing Acquisition in the Presence of TH

In order to find $\hat{\tilde{p}}_{rs}(t)$ from $r(t)$, we focus on segments of $r(t)$ that correspond to the subset of consecutive symbol pairs $(s[n], s[n-1])$ with $n \in \mathcal{G}_+(n; n_s)$; see, e.g., the segment of $r(t)$ corresponding to $y[n]$ in Fig. 2(b). For the other subset having $n \in \mathcal{G}_-(n; n_s)$, the corresponding segments of $r(t)$ experience a change of symbol signs every $T_s$, thus being unable to retain the symbol-independent $\tilde{p}_{rs}(t)$; see also the segment of $r(t)$ corresponding to $y[n+1]$ in Fig. 2(b). In fact, it is convenient to put all training symbols in $\mathcal{G}_+(n; n_s)$ (i.e., all 1s) as a preamble to estimate $n_s$, $\tilde{p}_{rs}(t)$, and other channel-dependent nuisance parameters, followed by a second block $\mathcal{G}_-(n; n_s)$ to be used as a post-amble to recover $n_f$. Identifying $\mathcal{G}_+(n; n_s)$ relies on the symbol-level timing offset parameter $n_s$, which we must obtain before proceeding to find $\hat{\tilde{p}}_{rs}(t)$.

To elaborate on the estimation of $n_s$ in the presence of TH, we revisit Proposition 1 to note that $n_s$ does not affect the symbol amplitudes in (6), regardless of TH. Indeed, for any general template $p_{rs}(t)$, (6) retains the same form as far as $n_s$ is concerned, except that $\nu_{f,\epsilon}$ does not simply depend on $n_f$ when TH is present. The GLRT approach in Section III, fortunately, relies on $\nu_{f,\epsilon}$ rather than $n_f$ to obtain the MLE of $n_s$. This observation indicates that $\hat{n}_s$ can be obtained using the derived GLRT rule even under TH for any correlation template satisfying Proposition 1. Specifically, $n_s$ can be estimated via a line search to maximize the objective function in either (15), (19), or (22), all of which involve only cross-correlation operations independent of $A_\epsilon$ or $n_f$. Based on our TS placement, we will use the first subset of (less than) $M_+$ training symbols to estimate $n_s$ as

$$\hat{n}_s = \arg \max_{n \in [0, N-M_+]} J_+(n_s, \mathbf{y}) = \arg \max_{n \in [0, N-M_+]} \frac{1}{\mathcal{E}_M^+} \left( \sum_{n=n_s}^{n_s+M_+-1} y[n] s[n-n_s] \right)^2. \quad (26)$$

Here, the sample vector $\mathbf{y}$ is generated by correlating the TH-dependent $r(t)$ with a general template $p_{rs}(t)$, e.g., $p_{rs}(t) = p_s(t)$ for simplicity.

Having acquired $n_s$, we can observe within $\mathcal{G}_+(n; n_s)$ a segment of $M_s T_s$-long received waveform $r_1(t)$, $t \in [(n_s+1)T_s, (n_s+M_s)T_s]$, which contains $s[n] = 1$, $\forall n$. For notational convenience, we introduce a window function $W_{T_s}(t)$, which equals 1 for $t \in [0, T_s)$ and 0 otherwise. With the remaining unknown timing offset $\tilde{\tau}_0 = n_f T_f + \epsilon$, we recall $r(t)$ in (4), and write $r_1(t)$ as

$$\begin{aligned} r_1(t) &= \sqrt{\mathcal{E}_s} \sum_{k=n_s+1}^{n_s+M_s-1} g_s(t - kT_s - \tilde{\tau}_0) + w(t) \Big|_{t=(n_s+1)T_s}^{(n_s+M_s)T_s} \\ &= \sqrt{\mathcal{E}_s} \sum_{k=n_s+1}^{n_s+M_s-1} \tilde{p}_{rs}(t - kT_s) \\ &\quad + \sum_{k=n_s+1}^{n_s+M_s-1} w(t) W_{T_s}(t - kT_s). \end{aligned} \quad (27)$$

Apparently, the noise-free part of $r_1(t)$ consists of $\tilde{p}_{rs}(t)$ replicas with spacing $T_s$. Hence, $\tilde{p}_{rs}(t)$ can be estimated from $r_1(t)$ by averaging over $M_s - 1$ consecutive $T_s$-long received waveform segments to yield a noisy template $\hat{\tilde{p}}_{rs}(t)$, $t \in [0, T_s)$ as

$$\hat{\tilde{p}}_{rs}(t) = \frac{1}{M_s - 1} \sum_{k=n_s+1}^{n_s+M_s-1} r_1(t + kT_s) W_{T_s}(t). \quad (28)$$

Being an unbiased sample mean of waveforms $\{r_1(t + kT_s)W_{T_s}(t)\}$, $\hat{\tilde{p}}_{rs}(t)$ asymptotically equals the corresponding ensemble mean $\tilde{p}_{rs}(t)$ as $M_s \to \infty$. As a result, any optimum estimator built upon the ideal correlation template $\tilde{p}_{rs}(t)$ will retain asymptotic optimality when the practical noisy template $\hat{\tilde{p}}_{rs}(t)$ in (28) is used instead.

Using $\hat{\tilde{p}}_{rs}(t)$, the CML parameter estimators in Section III can be directly applied to (25) in Proposition 2 to obtain the MLEs of $A_\epsilon$ and $n_f$ in the presence of TH. We summarize the overall procedure of GLRT-based timing synchronization under TH in Table I. This GLRT-based algorithm enjoys the same benefits as that in Section III in terms of symbol-rate sampling and low-complexity amplitude estimation without resorting to a line search over $n_f \in [0, N_f - 1]$. In addition, it is robust to TH by invoking a TH-dependent noisy template. To appreciate the TH-dependent feature of this noisy $\hat{\tilde{p}}_{rs}(t)$ template, we note that the TH code cannot be explicitly used during the acquisition phase because of the lack of code synchronization. A couple of remarks are in order.

TABLE I
ROBUST GLRT TIMING ACQUISITION USING NOISY TEMPLATE

| |
|---|
| I. Symbol-level timing offset estimation: |
| – generate $\{y[n]\}$ within $\mathcal{G}_+(n;n_s)$ using a simple template $p_s(t)$; |
| – estimate $n_s$ from (26); |
| II. Correlation with a noisy template: |
| – construct a noisy template $\hat{\tilde{p}}_{rs}(t)$ from (28); |
| – generate data samples using the noisy template: $y[n] = \int_{nT_s}^{(n+1)T_s} r(t)\hat{\tilde{p}}_{rs}(t - nT_s)dt$; |
| III. Frame-level timing acquisition: |
| – apply the data-aided timing acquisition algorithm (13) and (22) to obtain the MLE of $n_f$. |

*Remark 1:* The noisy template $\hat{\tilde{p}}_{rs}(t)$ is useful in a UWB correlator receiver even in the absence of TH or dense multipath effects. As shown in Appendix B, the ideal template $\tilde{p}_{rs}(t)$ maximizes the channel-dependent scalar $A_\epsilon$, an indicator of multipath energy capture, which in turn minimizes the timing

acquisition CRB in (18), thus improving estimation accuracy. This establishes that $\hat{\tilde{p}}_{rs}(t)$ is asymptotically optimum in the ML sense for symbol-by-symbol receiver processing.

*Remark 2:* Employing $\hat{\tilde{p}}_{rs}(t)$, Proposition 1 applies to all transmission formats utilizing $N_f$ equally spaced repetitive pulses to form a symbol, as long as there is no IFI in the received waveform. This class includes not only PAM- and PPM-based UWB but also direct-sequence (DS) UWB, operating in both dense multipath and low-scattering environments[3]. Similarly, Proposition 2 has merits in approximately modeling the correlator output of the same class of UWB transmissions, with the approximation entailing a small degree of IFI. IFI could arise when TH is used or when $T_f$ is set to be less than the channel delay spread to increase the date rate.

*Remark 3:* There is recent work on channel and timing estimation at low sampling rates based on the notion of finite innovation rates [9], [10]. Such work aims at recovering the delays and gains of (a few) dominant channel taps using a subspace-based harmonic retrieval approach operating in the frequency domain. As such, the sampling rates of innovation are lower than yet still comparable to the Nyquist rate. In the simulation curves in [10], considerable degradation of timing estimation performance can be witnessed when the sampling rate is $1/(8T_p)$. Our approach here aims at acquiring the time arrival of the first channel path without explicit channel estimation. The sampling rate of one sample per symbol ($1/T_s \ll 1/T_p$) is much lower than the Nyquist rate.

## V. Simulations

Computer simulations are performed to test the proposed CML timing acquisition algorithms. In all test cases, the propagation channels are generated randomly according to [19], where rays arrive in several clusters within an observation window. The cluster arrival times are modeled as Poisson variables with cluster arrival rate $\Lambda$. Returns within each cluster also arrive according to a Poisson process with arrival rate $\lambda$. The amplitude of each arriving ray is a real-valued random variable with a double-sided Rayleigh distribution having exponentially decaying mean square value with parameters $\Gamma$ and $\gamma$. Parameters of this channel model are chosen as $\Gamma = 30$ ns, $\gamma = 5$ ns, $1/\Lambda = 2$ ns, and $1/\lambda = 0.5$ ns. The diminishing tail of the multipath channel power profile is cut off to make the maximum delay spread of the multipath channel to be 99 ns. We select $p(t)$ as the second derivative of the Gaussian function, which has a pulse width $T_p = 1$ ns and normalized energy. The frame duration is chosen to be $T_f = 100$ ns. Each symbol duration contains $N_f = 25$ frames. In all cases, $N_\epsilon$ and $\epsilon$ are uniformly distributed over $[0, N_f - 1]$ and $[0, T_f)$, respectively. The chip duration is $T_c = 1.0$ ns and the TH code is chosen randomly over the range [0,90].

We present the acquisition performance of our GLRT-based timing offset estimators under different operating scenarios.

[3]In low-scattering environments, since the inherent multipath diversity provided by the channel is relatively small, the advantage of using noisy templates for collecting diversity gains at low cost has to be weighed against the noise enhancement effect incurred by lack of (computationally expensive yet noisy) channel estimates.

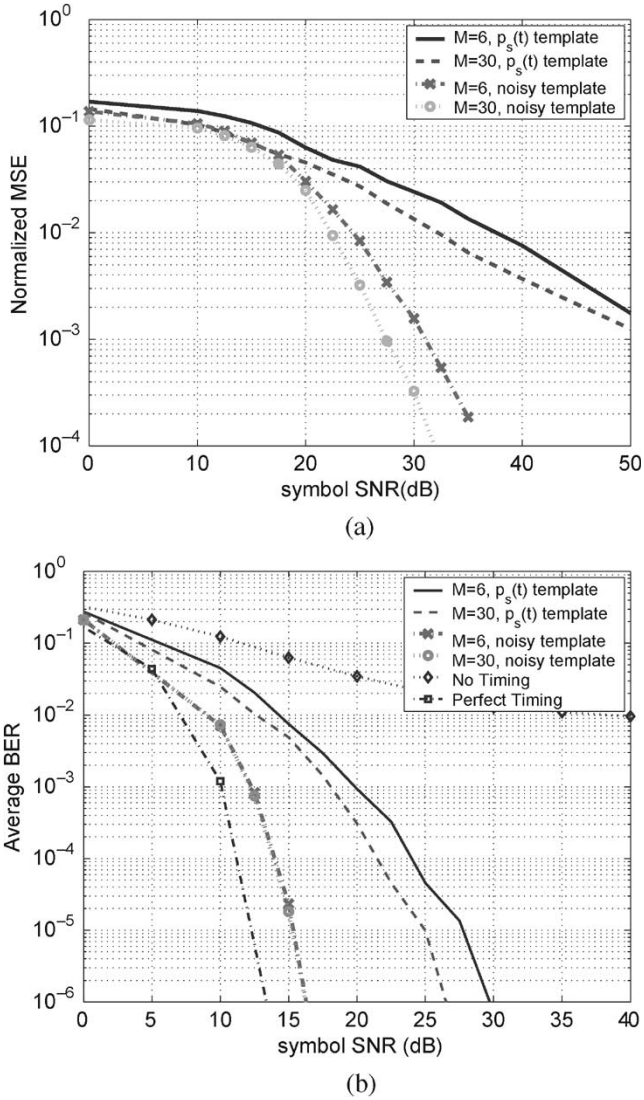


Fig. 3. Performance of GLRT timing acquisition with no TH and small tracking errors. (a) MSE. (b) BER.

Two correlation templates are compared: one is the simple suboptimal template $p_{rs}(t) = p_s(t)$, and the other is the asymptotically optimal template $p_{rs}(t) = \hat{\tilde{p}}_{rs}(t)$. Performance metrics of interest include the normalized acquisition estimation mean square error (MSE) $E\{|(\hat{n}_f - n_f)/N_f|^2\}$, and the BER when an optimum detector with perfect channel knowledge is available to recover information-bearing symbols, subject to residual timing errors.

Fig. 3 depicts the MSE and BER values versus SNR $\mathcal{E}_s/\sigma_w^2$ when TH is not employed and the pulse-level offset $\epsilon$ is small. Two different sizes of training symbol sequence, $M = 6$ and $M = 30$, are considered. Fig. 4 depicts the MSE and BER performance under large $\epsilon$ but no TH, while Fig. 5 depicts the case with TH and $\epsilon = 0$. With the template $p_s(t)$, the GLRT estimator in Section III-C can tolerate $\epsilon \neq 0$ to some degree, but is not robust to TH. Fig. 6 considers the acquisition performance with large $\epsilon$ errors in the presence of TH. The template $p_s(t)$ does not work well in this case, but the GLRT estimator in Section IV-B with the noisy template $\hat{\tilde{p}}_{rs}(t)$ is able to acquire timing at a reasonably low SNR. The noisy $\hat{\tilde{p}}_{rs}(t)$

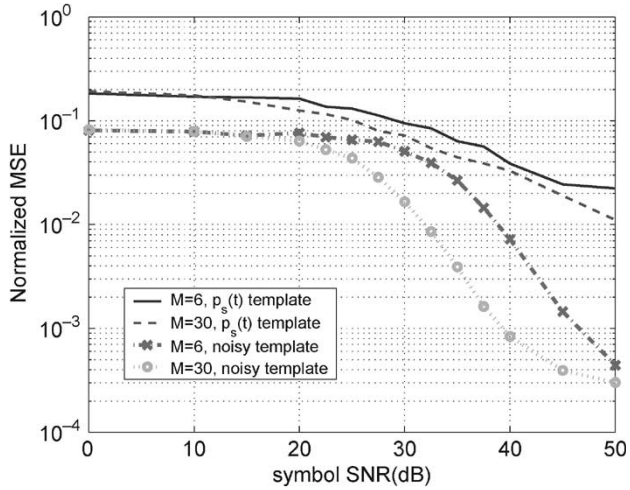


Fig. 4. MSE performance of robust GLRT timing acquisition with large tracking errors but no TH.

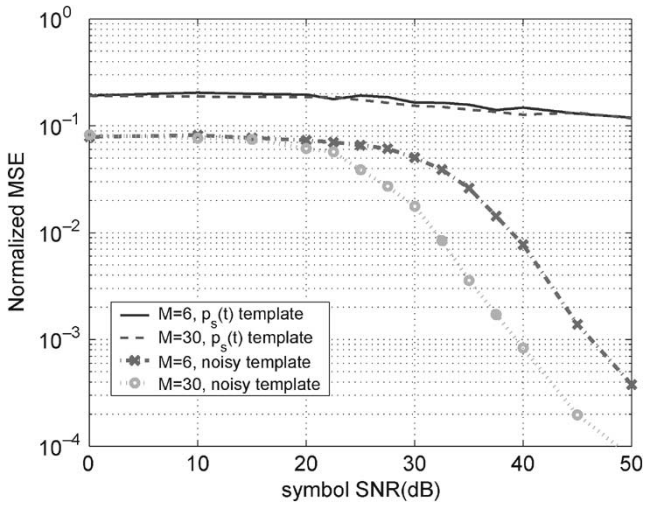


Fig. 5. MSE performance of robust GLRT timing acquisition with TH but no tracking errors.

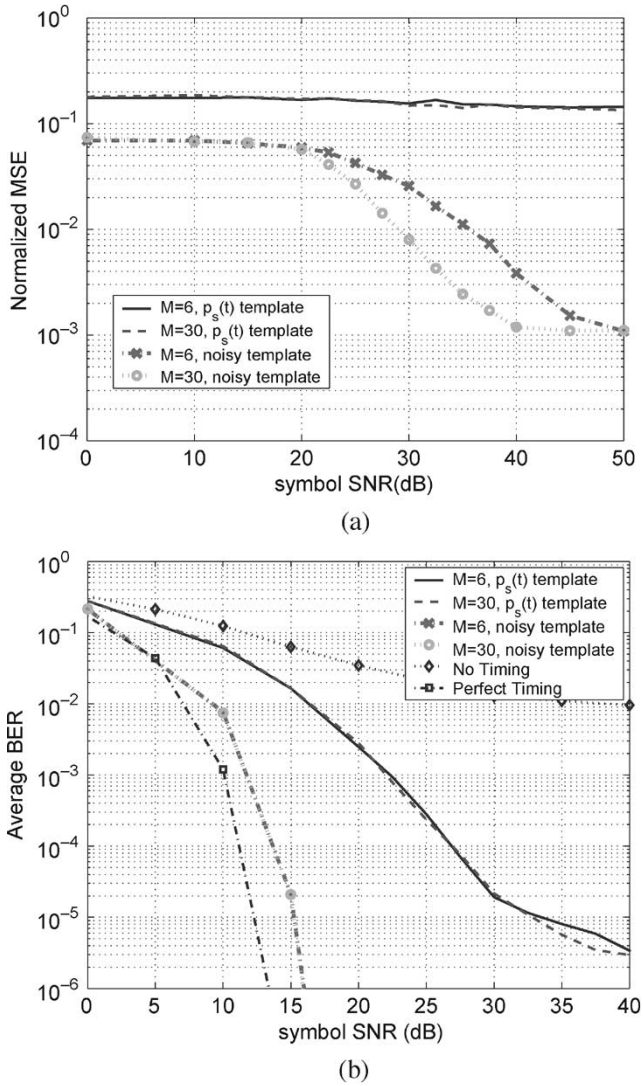


Fig. 6. Performance of robust GLRT timing acquisition with TH and large tracking errors. (a) MSE. (b) BER.

template considerably outperforms the $p_s(t)$ template in all the operating conditions tested because of its capability to benefit from the large diversity gain in dense multipath.

Since the unknown error $\epsilon$ has not been treated during the acquisition phase, there is a noise floor in the MSE curves in Figs. 4–6, which is caused by the bounded unknown $\lambda_\epsilon \in [0, 1]$ in (6) and (25). Nevertheless, tracking errors only have a small impact on BER in dense multipath channels [14]. As Figs. 3(b) and 6(b) illustrate, there are small BER gaps between our receivers using GLRT-based timing acquisition and an ideal receiver knowing the perfect timing information. Operating at a practical sampling rate of $1/T_s$, our GLRT timing acquisition algorithms not only enjoy very low computational complexity but also offer good acquisition accuracy when proper correlation templates are used.

## VI. Concluding Summary

Taking on a conditional maximum likelihood (CML) approach, this paper formulates the data-aided (DA) timing acquisition task for ultrawideband (UWB) communications as a generalized likelihood ratio test (GLRT) problem, where the effective discrete-time channel gains are viewed as nuisance parameters and estimated as by-products. Relying on symbol-rate samples, our synchronization solution boils down to an amplitude estimation problem, which permits a closed-form solution based on cross correlation among symbol-rate samples. This is in contrast to other digital synchronizers that require either chip-rate sampling or at least a line search. For competitive acquisition performance in dense multipath, the GLRT algorithms should be coupled with properly selected correlation templates that can effectively collect multipath energy in the presence of timing offsets. To this end, a noisy template is designed that not only offers asymptotically optimal estimation performance but also makes the GLRT robust to time hopping (TH). Performance bounds of DA acquisition have been established through Cramer–Rao bound (CRB), which we will explore in a companion paper to provide judicious training sequence design for improved acquisition performance and enhanced overall system capacity.

## APPENDIX A
## DISCRETE-TIME MODEL OF SYMBOL-RATE CORRELATOR OUTPUT SAMPLES

Consider a correlator receiver with a general correlation template $p_{rs}(t) := \sum_{j=0}^{N_f-1} p_{rf}(t-jT_f)$ made of $N_f$ identical $p_{rf}(t)$ with spacing $T_f$. Without knowing the mistiming, the receiver correlates the received waveform $r(t)$ [cf. (4)] with $p_{rs}(t)$ for every $T_s$ to generate samples $\{y[n]\}$, starting from $t=0$. Thus, $y[n] = \int_0^{T_s} r(t+nT_s)p_{rs}(t)dt = \sqrt{\mathcal{E}_s}\sum_{k=-\infty}^{\infty} s[k-n_s]\int_0^{T_s} g_s(t-kT_s-n_fT_f-\epsilon)\,p_{rs}(t)dt + w[n]$, where $w[n] := \int_0^{T_s} w(t+nT_s)p_{rs}(t)dt$ is the noise sample. Since $g_s(t)$ has a finite nonzero support on $t\in[0,T_s)$, the possible nonzero summands in $y[n]$ are associated only with either $k=n$ or $k=n-1$, yielding

$$\begin{aligned} y[n] = w[n] &+ \sqrt{\mathcal{E}_s}s[n-n_s-1]\int_0^{n_fT_f+\epsilon} g_s(t+T_s-n_fT_f-\epsilon)p_{rs}(t)dt \\ &+ \sqrt{\mathcal{E}_s}s[n-n_s]\int_{n_fT_f+\epsilon}^{T_s} g_s(t-n_fT_f-\epsilon)p_{rs}(t)dt. \end{aligned} \quad (29)$$

A key step in simplifying (29) is to express a finite-duration signal, namely, $g_s(t)$ in this case, in terms of its overlap with an infinite-duration version. To do so, let us introduce an extended aggregate channel $\bar{g}_s(t) := \sum_{j=-\infty}^{\infty} g(t-jT_f)$, which is periodic with period $T_f$. Noting that $g_s(t)$ overlaps with $\bar{g}_s(t)$ within $[0,T_s]$, we can replace $g_s(t)$ by $\bar{g}_s(t)$ in (29). Because $\bar{g}_s(t)$ is periodic for $t\in(-\infty,\infty)$, any arguments inside $\bar{g}_s(\cdot)$ that are integer multiples of $T_f$ can be simply omitted; thus, the integrands in (29) are independent of $n_f$ but still depend on $\epsilon$. As a result, the weights of the two contributing symbols become $\lambda_0 := \sqrt{\mathcal{E}_s}\int_{n_fT_f+\epsilon}^{T_s} \bar{g}_s(t-\epsilon)p_{rs}(t)dt$ and $\lambda_1 := \sqrt{\mathcal{E}_s}\int_0^{n_fT_f+\epsilon} \bar{g}_s(t-\epsilon)p_{rs}(t)dt$. We can thus simplify (29) to $y[n] = s[n-n_s]\lambda_0 + s[n-n_s-1]\lambda_1 + w[n]$. Next, we will show how $\lambda_0$ and $\lambda_1$ are related with the frame-level timing offset parameter $n_f$.

Let us start with $\lambda_1$. The following equalities hold after change of variables:

$$\begin{aligned} \lambda_1 &= \sqrt{\mathcal{E}_s}\int_0^{n_fT_f+\epsilon} \bar{g}_s(t-\epsilon)\sum_{j=0}^{N_f-1} p_{rf}(t-jT_f)dt \\ &= \sum_{j=0}^{N_f-1}\sqrt{\mathcal{E}_s}\int_{-jT_f}^{n_fT_f+\epsilon-jT_f} g_s(t+jT_f-\epsilon)p_{rf}(t)dt. \end{aligned} \quad (30)$$

Because $p_{rf}(t)$ is zero outside $t\in[0,T_f]$, each summand in (30) may contribute to $\lambda_1$ only when its integration range overlaps with $[0,T_f]$, reducing the possible values for the index $j$ to $j\in[0,n_f]$. Specifically

$$\begin{aligned} \lambda_1 = \sqrt{\mathcal{E}_s}\sum_{j=0}^{n_f-1}\int_0^{T_f} g_s(t+jT_f-\epsilon)p_{rf}(t)dt \\ + \sqrt{\mathcal{E}_s}\int_0^{\epsilon} g_s(t+n_fT_f-\epsilon)p_{rf}(t)dt. \end{aligned} \quad (31)$$

Because $g_s(t) := \sum_{i=0}^{N_f-1} g(t-iT_f)$ is made of $N_f$ replicas of $g(t)$, the first $n_f$ integrals in $\lambda_1$ are identical and we denote them as $A_\epsilon := \sqrt{\mathcal{E}_s}\int_0^{T_f} g(t+T_f-\epsilon)p_{rf}(t)dt$. The last term in $\lambda_1$ is equivalent to $\sqrt{\mathcal{E}_s}\int_0^{\epsilon} g(t+T_f-\epsilon)p_{rf}(t)dt$ because only the $j=(n_f-1)$th pulse $g(t-jT_f)$ in $g_s(t)$ falls within the integration range of $[0,\epsilon]$. It bears the same integrand as that in $A_\epsilon$, but the integration range is narrower. As such, the $\epsilon$-dependent scalar $\lambda_\epsilon := (1/A_\epsilon)\sqrt{\mathcal{E}_s}\int_0^{\epsilon} g(t+T_f-\epsilon)p_{rf}(t)dt$ is bounded within [0,1]. If there is no tracking error ($\epsilon=0$), then $\lambda_\epsilon = 0$. With these definitions, (31) can be expressed as $\lambda_1 = A_\epsilon(n_f+\lambda_\epsilon)$.

Similar derivations apply to $\lambda_0$, yielding $\lambda_0 = A_\epsilon(N_fn_f - n_f - \lambda_\epsilon)$. Together, we reach

$$\begin{aligned} y[n] = A_\epsilon\,(s[n-n_s](N_f-n_f-\lambda_\epsilon) \\ + s[n-n_s-1](n_f+\lambda_\epsilon)) + w[n]. \end{aligned} \quad (32)$$

In (32), the unknown channel impulse response $g(t)$ is contained in the scalars $A_\epsilon$ and $\lambda_\epsilon$ in a discrete-time form.

## APPENDIX B
## SAMPLE MODEL USING AN IDEAL TEMPLATE UNDER MISTIMING

To find the output sample model of a correlator using the ideal template $\tilde{p}_{rs}(t)$ in (24), we replace $p_{rs}(t)$ by $\tilde{p}_{rs}(t)$ in (29) to reach the noise-free component $\bar{y}(n)$ of each sample, i.e.,

$$\begin{aligned} \bar{y}(n) &= \sqrt{\mathcal{E}_s}s[n-n_s]\int_{n_fT_f+\epsilon}^{T_s} g_s^2(t-n_fT_f-\epsilon)dt \\ &\quad + \sqrt{\mathcal{E}_s}s[n-n_s-1]\int_0^{n_fT_f+\epsilon} g_s^2(t-n_fT_f-\epsilon+T_s)dt \\ &= \sqrt{\mathcal{E}_s}s[n-n_s]\int_0^{T_s-(n_fT_f+\epsilon)} g_s^2(t)dt \\ &\quad + \sqrt{\mathcal{E}_s}s[n-n_s-1]\int_{T_s-(n_fT_f+\epsilon)}^{T_s} g_s^2(t)dt. \end{aligned} \quad (33)$$

$$
\begin{aligned}
\xi_{\tilde{\tau}_0} &= \sqrt{\mathcal{E}_s} \int_{(N_f-n_f)T_f-\epsilon}^{N_fT_f} \sum_{i=0}^{N_f-1} g(t-iT_f-c_iT_c) \sum_{j=0}^{N_f-1} g(t-jT_f-c_jT_c)dt \\
&= \sqrt{\mathcal{E}_s} \sum_{i=N_f-n_f-2}^{N_f-1} \int_{(N_f-n_f-i)T_f-c_iT_c-\epsilon}^{(N_f-i)g(t+T_f-(c_{i-1}-c_i)T_c)T_f-c_iT_c} \sum_{j=i-1}^{i+1} g(t)g\left(t-(j-i)T_f-(c_j-c_i)T_c\right)dt \\
&= \sqrt{\mathcal{E}_s} \underbrace{\sum_{i=N_f-nf}^{N_f-1} \int_0^{T_f} g^2(t)dt}_{\mathcal{E}_{gf}n_f} + \sqrt{\mathcal{E}_s} \underbrace{\left[ \sum_{i=N_f-n_f-2}^{N_f-n_f-1} \int_{(N_f-n_f-i)T_f-c_iT_c-\epsilon}^{T_f} g^2(t)dt - \int_{T_f-c_{N_f-1}T_c}^{T_f} g^2(t)dt \right]}_{\mathcal{E}_{gf}\lambda_\epsilon} \\
&\quad + \sqrt{\mathcal{E}_s} \sum_{i=N_f-n_f}^{N_f-2} \int_0^{T_f} g(t)\left[g\left(t-T_f-(c_{i+1}-c_i)T_c\right)+g\left(t+T_f-(c_{i-1}-c_i)T_c\right)\right]dt \\
&\quad + \sqrt{\mathcal{E}_s} \sum_{i=N_f-n_f-2}^{N_f-n_f-1} \int_{(N_f-n_f-i)T_f-c_iT_c-\epsilon}^{T_f} g(t)\left[g\left(t-T_f-(c_{i+1}-c_i)T_c\right)+g\left(t+T_f-(c_{i-1}-c_i)T_c\right)\right]dt \\
&\quad + \sqrt{\mathcal{E}_s} \int_0^{T_f-c_{N_f-1}T_c} g(t)g\left(t+T_f-\left(c_{N_f-2}-c_{N_f-1}\right)T_c\right)dt \\
&= \sqrt{\mathcal{E}_s}\mathcal{E}_{gf}(n_f+\lambda_\epsilon+\zeta_{nf,\epsilon})
\end{aligned} \tag{34}
$$

We first derive the effective channel-dependent amplitude $A_\epsilon$ attained by such a correlation template, [i.e., (34) shown at the top of the page]. Analogous to the signal structure in (32), we observe that $A_\epsilon$ is equivalent to the sample amplitude when there is no modulation or change of symbol signs, while the portion of sample amplitude contributed from $s[n-n_s-1]$ reflects the frame-level acquisition error. Based on this observation, we deduce that the effective gain $A_\epsilon$ in (33) is given by $A_\epsilon = (1/N_f)\,\bar{y}(n)|_{s[n-n_s]=s[n-n_s-1]=1} = (1/N_f)\sqrt{\mathcal{E}_s}\int_0^{T_s} g_s^2(t)\,dt$, where $\mathcal{E}_{gs} := \int_0^{T_s} g_s^2(t)dt$ represents the maximum energy collected within a symbol when free of noise, simply because the received (unknown) waveform template $g_s(t)$ itself is used as the correlation template to perform optimum matched filtering. The result on $A_\epsilon$ can be intuitively understood from Fig. 2. Since the template matches exactly the received waveform and the integration range is the same as the waveform period $T_s$, such a template collects the energy of an entire symbol.

Next, we focus on the effective channel-dependent weighting gain of $s[n-n_s-1]$ while the gain of $s[n-n_s]$ is simply given by $A_\epsilon$ minus that of $s[n-n_s-1]$. The quantity of interest is $\xi_{\tilde{\tau}_0} := \sqrt{\mathcal{E}_s}\int_{T_s-(n_fT_f+\epsilon)}^{T_s} g_s^2(t)dt$. Defining the pulse energy after multipath spreading as $\mathcal{E}_{gf} := \int_0^{T_f} g^2(t)dt$, the manipulations in (34) stand.

Using (34) and scaling it by $1/\sqrt{\mathcal{E}_{gf}}$ to keep the noise variance at $\sigma_w^2$, the symbol-rate signal model in (33) becomes

$$
\begin{aligned}
y[n] &= \sqrt{\mathcal{E}_s\mathcal{E}_{gf}}s[n-n_s](N_f-n_f-\lambda_\epsilon-\zeta_{n_f,\epsilon}) \\
&\quad + \sqrt{\mathcal{E}_s\mathcal{E}_{gf}}s[n-n_s-1](n_f+\lambda_\epsilon+\zeta_{n_f,\epsilon}) + w[n].
\end{aligned} \tag{35}
$$

The following observations can be made.

- The no-TH case ($\{c_i=0\}$): It holds that $\mathcal{E}_{gs} = N_f\mathcal{E}_g$ and $\zeta_{n_f,\epsilon}=0$ because the latter involves correlating $g(t)$ with $g(t\pm T_f)$ whereas the nonzero support of $g(t)$ is $T_f$. Furthermore, $\lambda_\epsilon$ is reduced to $\lambda_\epsilon = (1/\mathcal{E}_{gf})\int_0^\epsilon g^2(t)dt \le 1$, corroborating with (6).
- The TH case: Due to the IFI induced by pulse overlapping, $\zeta_{n_f,\epsilon}$ is no longer zero; thus, the $\lambda_\epsilon$ term in (6) should be replaced by $\tilde{\lambda}_\epsilon := \lambda_\epsilon + \zeta_{n_f,\epsilon}$ to reach (25). As long as IFI is small, the value of $\zeta_{n_f,\epsilon}$ in (35) is relatively small, especially when $T_p \ll T_f$ and $N_f$ is large. Besides, the channel taps in the overlapping region do not match and could be faded independently; therefore, the impact of their correlation in the fading case is trivial.

## REFERENCES


[1] R. A. Scholtz, "Multiple access with time-hopping impulse radio," in *Proc. IEEE Military Communications (Milcom) Conf.*, Boston, MA, Oct. 1993, pp. 447–450.

[2] C. J. Le Martret and G. B. Giannakis, "All-digital impulse radio for wireless cellular systems," *IEEE Trans. Commun.*, vol. 50, no. 9, pp. 1440–1450, Sep. 2002.

[3] W. M. Lovelace and J. K. Townsend, "The effects of timing jitter and tracking on the performance of impulse radio," *IEEE J. Sel. Areas Commun.*, vol. 20, no. 9, pp. 1646–1651, Sep. 2002.

[4] E. A. Homier and R. A. Scholtz, "Rapid acquisition of ultra-wideband signals in the dense multipath channel," in *Proc. IEEE Conf. UWB Systems & Technologies*, Baltimore, MD, May 2002, pp. 245–250.

[5] J. Y. Lee and R. A. Scholtz, "Ranging in a dense multipath environment using a UWB radio link," *IEEE J. Sel. Areas Commun.*, vol. 20, no. 12, pp. 1677–1683, Dec. 2002.

[6] R. Blazquez, P. Newaskar, and A. Chandrakasan, "Coarse acquisition for ultra wideband digital receivers," in *Proc. Int. Conf. Acoustics, Speech, and Signal Processing*, Hong Kong, Apr. 2003, pp. IV.137–IV.140.
[7] A. R. Forouzan, M. Nasiri-Kenari, and J. A. Salehi, "Performance analysis of ultra-wideband time-hopping spread spectrum multiple-access systems: Uncoded and coded systems," *IEEE Trans. Wireless Commun.*, vol. 1, no. 4, pp. 671–681, Oct. 2002.
[8] R. Fleming, C. Kushner, G. Roberts, and U. Nandiwada, "Rapid acquisition for ultra-wideband localizers," in *Proc. IEEE Conf. UWB Systems & Technologies*, Baltimore, MD, May 2002, pp. 245–250.
[9] I. Maravic, J. Kusuma, and M. Vetterli, "Low-sampling rate UWB channel characterization and synchronization," *J. Commun. Netw.*, vol. 5, no. 4, pp. 319–327, Dec. 2003.
[10] J. Kusuma, I. Maravic, and M. Vetterli, "Sampling with finite innovation rate: Channel and timing estimation in UWB and GPS," in *Proc. Int. Conf. Communications*, Anchorage, AK, May 2003, vol. 5, pp. 3540–3544.
[11] L. Yang, Z. Tian, and G. B. Giannakis, "Non-data-aided timing acquisition of UWB signals using cyclostationary," in *Proc. Int. Conf. Acoustics, Speech, and Signal Processing*, Hong Kong, Apr. 2003, pp. IV.121–IV.124.
[12] Z. Tian, L. Yang, and G. B. Giannakis, "Symbol timing estimation in ultra-wideband communications," in *Proc. Asilomar Conf. Signals, Systems and Computers*, Pacific Grove, CA, Nov. 2002, pp. 1924–1928.
[13] V. Lottici, A. D'Andrea, and U. Mengali, "Channel estimation for ultra-wideband communications," *IEEE J. Sel. Areas Commun.*, vol. 20, no. 12, pp. 1638–1645, Dec. 2002.
[14] Z. Tian and G. B. Giannakis, "BER sensitivity to timing offset in UWB impulse radios," *IEEE Trans. Signal Process.*, 2004. (to be published).
[15] ——, "A GLRT approach to data-aided timing acquisition in UWB radios–Part II: Training sequence design," *IEEE Trans. Wireless Commun.*, vol. 4, no. 6, Nov. 2005.
[16] R. Hoctor and H. Tomlinson, "Delay-hopped transmitted-reference RF communications," in *IEEE Conf. UWB Systems & Technologies*, Baltimore, MD, May 2002, pp. 265–269.
[17] L. Yang and G. B. Giannakis, "Low-complexity training for rapid timing acquisition in ultra-wideband communications," in *Proc. Global Telecommunications (Globecom) Conf.*, San Francisco, CA, Dec. 1–5, 2003, vol. 2, pp. 769–773.
[18] S. M. Kay, *Fundamentals of Statistical Signal Processing: Vol. II–Detection Theory*. Englewood Cliffs, NJ: Prentice-Hall, Dec. 1998.
[19] A. A. M. Saleh and R. A. Valenzuela, "A statistical model for indoor multipath propagation," *IEEE J. Sel. Areas Commun.*, vol. SAC-5, no. 2, pp. 128–137, Feb. 1987.
[20] J. Riba, J. Sala, and G. Vazquez, "Conditional maximum likelihood timing recovery: Estimators and bounds," *IEEE Trans. Signal Process.*, vol. 49, no. 4, pp. 835–850, Apr. 2001.

**Zhi Tian** (M'98–S'98–M'00) received the B.E. degree in electrical engineering (automation) from the University of Science and Technology of China, Hefei, in 1994, the M.S. and Ph.D. degrees from George Mason University (GMU), Fairfax, VA, in 1998 and 2000, respectively.

From 1995 to 2000, she was a Graduate Research Assistant at the Center of Excellence in Command, Control, Communications and Intelligence (C3I), GMU. Since August 2000, she has been an Assistant Professor at the Department of Electrical and Computer Engineering, Michigan Technological University, Houghton. Her current research focuses on signal processing for wireless communications, particularly on ultrawideband systems.

Dr. Tian serves as an Associate Editor for the IEEE TRANSACTIONS ON WIRELESS COMMUNICATIONS. She was the recipient of the 2003 National Science Foundation (NSF) CAREER award.

**Georgios B. Giannakis** (S'84–M'86–SM'91–F'97) received the Diploma in electrical engineering from the National Technical University of Athens, Greece, in 1981, and the M.Sc. degree in electrical engineering, the M.Sc. degree in mathematics, and the Ph.D. degree in electrical engineering from the University of Southern California (USC), Los Angeles, in 1983, 1986, and 1986, respectively.

After lecturing for one year at USC, he joined the University of Virginia, Charlottesville, in 1987, where he became a Professor of electrical engineering in 1997. Since 1999, he has been a Professor at the Department of Electrical and Computer Engineering, University of Minnesota, Minneapolis, where he now holds an ADC Chair in Wireless Telecommunications. His general interests span the areas of communications and signal processing, estimation and detection theory, time-series analysis, and system identification—subjects on which he has published more than 220 journal papers, 380 conference papers, and two edited books. Current research focuses on transmitter and receiver diversity techniques for single- and multiuser fading communication channels, complex-field and space-time coding, multi-carrier ultrawide band wireless communication systems, cross-layer designs, and sensor networks.

Dr. Giannakis is the (co)recipient of six paper awards from the IEEE Signal Processing (SP) and Communications Societies (1992, 1998, 2000, 2001, 2003, and 2004). He also received the IEEE-Signal Processing Society's Technical Achievement Award in 2000 and European Association for Signal, Speech and Image Processing (EURASIP) Technical Achievement Award in 2005. He served as Editor-in-Chief for the IEEE SIGNAL PROCESSING LETTERS, as Associate Editor for the IEEE TRANSACTIONS ON SIGNAL PROCESSING and the IEEE SIGNAL PROCESSING LETTERS, as Secretary of the Signal Processing Conference Board, as member of the Signal Processing Publications Board, as member and Vice-Chair of the Statistical Signal and Array Processing Technical Committee, as Chair of the Signal Processing for Communications Technical Committee, and as a member of the IEEE Fellows Election Committee. He has also served as a member of the IEEE-Signal Processing Society's Board of Governors, the Editorial Board for the PROCEEDINGS OF THE IEEE, and the Steering Committee of the IEEE TRANSACTIONS ON WIRELESS COMMUNICATIONS.